THE JOURNAL OF BIOLOGICAL CHEMISTRY Vol. 276, No. 29, Issue of July 20, pp. 27535–27540, 2001
Printed in U.S.A.

Crystal Structure of the Dimeric C-terminal Domain of TonB Reveals a Novel Fold*

Received for publication, March 29, 2001, and in revised form, April 26, 2001
Published, JBC Papers in Press, April 27, 2001, DOI 10.1074/jbc.M102778200

Changsoo Chang‡§, Alexandre Mooser§¶, Andreas Plückthun¶‖, and Alexander Wlodawer‡

From the ‡Macromolecular Crystallography Laboratory, NCI, National Institutes of Health, Frederick, Maryland 21702 and the ¶Biochemisches Institut der Universität Zürich, Winterthurerstrasse 190, Zürich CH-8057, Switzerland

The TonB-dependent complex of Gram-negative bacteria couples the inner membrane proton motive force to the active transport of iron·siderophore and vitamin B_{12} across the outer membrane. The structural basis of that process has not been described so far in full detail. The crystal structure of the C-terminal domain of TonB from *Escherichia coli* has now been solved by multi-wavelength anomalous diffraction and refined at 1.55-Å resolution, providing the first evidence that this region of TonB (residues 164–239) dimerizes. Moreover, the structure shows a novel architecture that has no structural homologs among any known proteins. The dimer of the C-terminal domain of TonB is cylinder-shaped with a length of 65 Å and a diameter of 25 Å. Each monomer contains three β strands and a single α helix. The two monomers are intertwined with each other, and all six β-strands of the dimer make a large antiparallel β-sheet. We propose a plausible model of binding of TonB to FhuA and FepA, two TonB-dependent outer-membrane receptors.

The outer membrane (OM[1]) of Gram-negative bacteria constitutes a permeability barrier, protecting the cell against a variety of toxic agents. The lipopolysaccharides located in the outer leaflet of the OM confer to the bacteria a polar and negatively charged surface, restricting the cellular uptake of toxic organic molecules and detergents such as bile salts, the detergents in the gut. However, although the OM is an effective protective barrier against harmful environmental components, it also represents an additional obstacle for the uptake of nutrients, which can be circumvented in three ways. While small hydrophilic nutrients (<600 Da) enter the periplasm by simple diffusion through porins in a non-selective manner (1), larger molecules are taken up by pores with an internal binding site for the ligand (such as LamB) in a stereospecific and selective manner (2) and can subsequently enter the cytoplasm by a variety of transporters located in the inner membrane (3). A few nutrients, notably iron and vitamin B_{12}, need to be taken up into the periplasm against their concentration gradients. For this purpose, a complex consisting of TonB, ExbB, and ExbD couples the inner membrane proton motive force (pmf) to the active transport of iron siderophores and vitamin B_{12} across the OM through specialized porins. Recently, crystal structures were solved for two TonB-dependent receptors, FepA and FhuA (4–6). Like all other known porins, they are β-barrels, but unlike the other porin structures they have much larger interiors, which are almost completely obscured by a protein domain sitting inside the barrel (termed the "cork" or "hatch region"), which is encoded within the N-terminal segment of either protein.

Iron uptake into bacteria is initiated by the binding of the iron·siderophore complex to the high affinity OM receptor. The dissociation constant is around 100–200 nM (7, 8). An electron spin resonance study (9), later rationalized by three-dimensional structural models (4–6), has shown that this event triggers conformational changes in the OM receptor. This might allow TonB to contact specific regions on the receptor. It appears that "energized" TonB is then able to deliver its energy to the receptor, resulting in ligand translocation into the periplasm (10, 11). ExbB·ExbD are implicated in the recycling of TonB, from its high affinity OM receptor association to a high affinity inner membrane association (12, 13). The structural changes in this whole process have remained almost completely unclear.

TonB of *Escherichia coli* is a protein consisting of 239 amino acids. Homologs of TonB have been found in several Gram-negative species (14). The N terminus is in the cytoplasm; the protein is anchored in the inner membrane by its uncleaved N-terminal signal sequence (15, 16), and most of the protein extends into the periplasm. The membrane anchor sequence contains a set of highly conserved residues located on one face of the α-helix (SHLS motif). The sequence S*XXX*H (where *X* is any amino acid) has been defined as the minimal structural requirement for the coupling of TonB to the electrochemical gradient of the inner membrane (17). The amino acid sequence of TonB contains a long central region with a high percentage of proline residues between residues 70 and 102 (17%), which is thought to confer to TonB the conformational rigidity and extended shape necessary to span the periplasm, and thereby to allow the C-terminal domain to contact the receptor embedded in the OM (18). Mutational studies have defined the last 48 residues as being essential to make contact with the OM receptor (19).

TonB forms a complex in the inner membrane with ExbB and ExbD (13), two membrane proteins that could potentially act as proton translocators. ExbB is homologous to the protein MotA, and ExbD has a similar topology as MotB, both of which are thought to exploit the proton gradient to drive the bacterial flagellum. ExbB has been proposed to modulate the conformation of TonB (20), as well as mediate its recycling (12, 13), but it has remained an enigma as to what these structural changes

* The costs of publication of this article were defrayed in part by the payment of page charges. This article must therefore be hereby marked "*advertisement*" in accordance with 18 U.S.C. Section 1734 solely to indicate this fact.

§ Both authors contributed equally to this work.

‖ To whom correspondence should be addressed: Biochemisches Institut der Universität Zürich, Winterthurerstrasse 190, CH-8057 Zürich, Switzerland. Tel.: 41-1-635-5570; Fax: 41-1-635-5712; E-mail: plueckthun@biocfebs.unizh.ch.

[1] The abbreviations used are: OM, outer membrane; pmf, proton motive force; Mes, 4-morpholinoethanesulfonic acid; r.m.s., root mean square; IEX, ion exchange chromatography; IMAC, immobilized metal ion affinity chromatography; MAD, multiwavelength anomalous diffraction.

TABLE I
Data collection statistics

	Remote 2	Remote 1	Peak	Inflection
Wavelength (Å)	0.9800	0.9163	0.9196	0.9199
Resolution (Å)	20–1.55	20–2.0	20–2.0	20–2.0
Total reflections	138,987	80,451	81,133	58,622
Unique reflections	21,518	19,195	19,199	19,128
		(F+ and F− separated)	(F+ and F− separated)	(F+ and F− separated)
Completeness (%) (last shell)	96.8 (80.2)	99.6 (98.3)	99.6 (97.6)	99.1 (96.5)
R_{merge}	2.7 (11.0)	2.3 (4.1)	2.5 (4.3)	1.7 (4.2)

might be. Cross-linking studies have suggested the regions through which TonB might interact with its partners in the inner membrane: The contact with ExbB is mediated by the signal anchor (20), whereas the residues responsible for the interaction with ExbD are unknown (21).

TonB and its associated proteins ExbB·ExbD thus play the role of an energy-transducing complex, coupling the electrochemical proton gradient of the inner membrane to active import processes across the OM (13, 22). The energy is provided by the proton motive force (10, 23, 24). For the transduction process to occur, the C-terminal domain of TonB must contact the OM receptor. Based on genetic (25, 26), cross-linking (19, 27–29), and affinity chromatography (30) studies, a recognition site has been suggested on the receptor, the TonB box, a hydrophobic stretch of seven amino acids, which is highly conserved in all the TonB-dependent OM receptors (31). A recent study resulted in the proposal that the conformation rather than the sequence of the TonB box is important for the recognition process between TonB and the receptor (19). Moreover, it has been hypothesized that other regions of both interacting partners are also involved (27). Most strikingly, TonB dependence is maintained if the complete cork domain is deleted (32, 33), including the TonB box. It follows that the recognition site cannot be limited to the TonB box.

A number of phages and colicins have exploited the TonB·ExbB·ExbD system for gaining entry into bacteria (34). A similar system, TolQRA, has also been described as allowing entry for other phages and colicins (34). The cellular function of the TolQRA system has remained enigmatic, and its deletion leads to a leaky phenotype (although no such effect is caused by the deletion of TonB·ExbB·ExbD). Nevertheless, both systems can partially complement each other (35). We have recently described the crystal structure of the C-terminal domain of TolA (36), and we became interested in finding out whether any structural similarity might exist between the C-terminal domains of both TonB and TolA.

In this paper, we present the crystal structure of the C-terminal domain of TonB at 1.55-Å resolution and show that this protein exhibits a novel fold that is without homology to any known structures. Moreover, we provide the first evidence that the C-terminal domain of TonB forms a tightly intertwined dimer.

EXPERIMENTAL PROCEDURES

Protein Expression and Purification—The sequence encoding residues 155–239 of *tonB* from *E. coli* strain JM83 was polymerase chain reaction-amplified and cloned into the plasmid pAT37 (based on pQE30 from Qiagen). pAT37 codes for protein D (gpD) from bacteriophage λ with an N-terminal His-tag, under control of the T5 promoter (37). The *tonB* gene was fused to the C terminus of gpD, with an enterokinase cleavage site engineered by the polymerase chain reaction in between the two proteins. Recombinant bovine enterokinase (purchased from Invitrogen) cleaves after the sequence Asp-Asp-Asp-Asp-Lys. The recombinant protein was expressed overnight at 30 °C in *E. coli* XL1-Blue, after induction with 1 mM isopropyl-β-D-thio-galactopyranoside. Cells were lysed with a French press and, after centrifugation, the gpD-TonB fusion protein remained in the soluble fraction. The undigested fusion was purified at pH 8.0, using the coupled IMAC-IEX (cation exchange) protocol (38) on a BIOCAD-60 workstation. After dialysis against 50 mM Tris, pH 8.0, 1 mM $CaCl_2$, 0.1% Tween 20, the cleavage reaction was performed at room temperature for 4 h, using 1 unit per mg of fusion of the recombinant bovine enterokinase (Invitrogen). The solution was then dialyzed against 50 mM Mes/Hepes/acetate buffer, pH 8.0. Removal of gpD and enterokinase was again achieved with the coupled IMAC-IEX (cation exchange) protocol, based on the different pI of TonB, gpD, and enterokinase.

Crystallization and Structure Solution—The C-terminal domain of TonB was dialyzed against 20 mM Tris buffer at pH 7.5 and was concentrated to 15 mg/ml. Crystallization was performed by the hanging-drop vapor diffusion method at 22 °C. Crystal screen I (Hampton Research) was used for the initial screening. Small, rod-shaped crystals were found under conditions 6, 19, 27, and 36. The final refined crystallization conditions were 28–30% polyethylene glycol 3350, 0.1 M Tris buffer at pH 7.5, 50–100 mM $CaCl_2$. After refinement of the conditions, crystals were grown to the size of 0.3–0.5 mm. When a crystal was picked up from a droplet, the diffraction pattern showed split spots or high mosaicity. To improve their quality, crystals were moved from the droplet to a well containing mother liquor and stored for more than 1 day. Such treatment both increased the resolution of diffraction and lowered the mosaicity. TonB crystals were found to belong to the orthorhombic space group $P2_12_12$ with the unit cell parameters $a = 63.78$ Å, $b = 86.34$ Å, $c = 26.56$ Å. The asymmetric unit contains two molecules, and the V_M value is 1.89 Å^3/Da (solvent content 35%).

The structure of TonB was solved by derivatization with Br^- ions (39, 40). To prepare a crystal for this procedure, it was soaked for 50 s in a solution containing 1.0 M KBr in addition to the crystallization buffer. Subsequently, the crystal was picked up with a nylon loop (Hampton Research) and was flash-frozen in a nitrogen stream. All data sets were collected at 100 K using the ADSC Quantum 4 charge-coupled device detector on the synchrotron beamline X9B at the National Synchrotron Light Source, Brookhaven National Laboratory, Upton, NY. The bromine fluorescence edge was scanned to determine the energy of the inflection, peak, and remote points. Three data sets were measured at 2.0-Å resolution to provide all information necessary for a multiwavelength anomalous diffraction (MAD) experiment. In addition, a data set extending to 1.55 Å was obtained for the purpose of structure refinement. Data were integrated and scaled using the HKL2000 program suite (41). Data collection statistics are summarized in Table I.

Four Br^- sites were found by both direct and Patterson methods and were refined using the program SOLVE (42), utilizing three data sets corresponding to the peak, inflection, and remote wavelengths, in the resolution range 10–2.5 Å. These sites were also confirmed with the program SHELXD (43). The phases from SOLVE were modified and extended to 1.55 Å using the program DM (44) in the CCP4 program suite (45), with the solvent content set at 25%. The mean figure of merit of the phase set was 0.608 for the 10–2.5 Å data after SOLVE, and 0.489 for 20–1.55 Å after DM (0.780 for 20–2.5 Å). The initial model was built using the automatic model-building option of the program ARP/wARP (46) with the full-DM phase set as input. The model was rebuilt with the program O (47) using either electron density maps based on the combination of the MAD and model phases, or straight $2F_o - F_c$ maps. The combined phase set was obtained using SIGMAA in the CCP4 program package. After each cycle of rebuilding, the model was refined using SHELXL (48) at the resolution range of 20 to 1.55 Å, without applying any non-crystallographic (NCS) restraints, as the latter prevented proper convergence. Eight full cycles of remodeling and refinement were performed, with the refinement of individual anisotropic *B*-factors for all atoms initiated in cycle six. In addition to protein atoms, 219 water molecules and four bromide ions have been added to the model. The *R*-value for all reflections between 20 and 1.55 Å is 16.0% (R_{free} 23.0%). The geometrical properties of the model were assessed by the

program PROCHECK (49), and the secondary structure elements were assigned by the program PROMOTIF (50). The figures were prepared with Molscript (51) or Bobscript (52) and rendered with Raster3D (53).

RESULTS

The crystal structure of the C-terminal domain of TonB has been determined by multiwavelength anomalous diffraction, and has been refined using SHELXL at 20–1.55 Å, yielding a model with low *R*-factor and excellent stereochemistry. The refinement statistics and the indicators of model quality are listed in Table II. The electron density maps (both the combined map utilizing the phases of the MAD data and of the model, and the final $2F_o - F_c$ map) are generally of excellent quality (Fig. 1). However, both maps are poorly defined in the neighborhood of residues 194–201. In this region, *B*-factors of all atoms are relatively high, indicating extensive flexibility of the polypeptide chain. Some disorder is also present at both termini of each molecule. Residues that are not visible in the maps include the first ten N-terminal amino acids of our construct (residues 155–164), as well as the last one or two residues on the C terminus (residues 238 and 239 of molecule A, and 239 of molecule B). The electron density of the remaining parts of the protein is very well defined. The mean positional error in atomic coordinates as estimated by the Luzzati plot is 0.16 Å. All non-glycine and non-proline residues of the model lie either in the most favorable region or in the additionally allowed region of the Ramachandran plot.

TABLE II
Refinement statistics for the final coordinates of the C-terminal domain of TonB

Resolution range	20.0–1.55 Å
Unique reflections used	20,365
R_{cryst}	16.0%
R_{free}	23.0% (5% test set)
r.m.s. deviations from ideality	
Bond lengths	0.009 Å
Angles	0.028 Å
Non-zero chiral volumes	0.054 Å^3
Zero chiral volumes	0.047 Å^3
Number of amino acid residues	73 + 74
Number of protein atoms	578 + 586
Number of heteroatoms	4
Number of solvent atoms	219

The C-terminal domain of TonB is cylinder-shaped with the length of 65 Å, and the diameter of 25 Å, with two protein chains forming a single compact entity. Each chain is rich in β-strands (~50% of the secondary structure) with much more limited extent (~15%) of residues found in helical conformation (either α-helix or 3_{10} helix). Each monomer contains three β-strands (strand S1, residues 169–182; S2, 188–194; and S3, 221–236) and one α-helix (residues 200–210 in molecule A, and 200–211 of molecule B). In addition, a short 3_{10} helix includes residues 211–213 of molecule A. All six β-strands make a large antiparallel β-sheet. The β-strand S3 of each monomer is

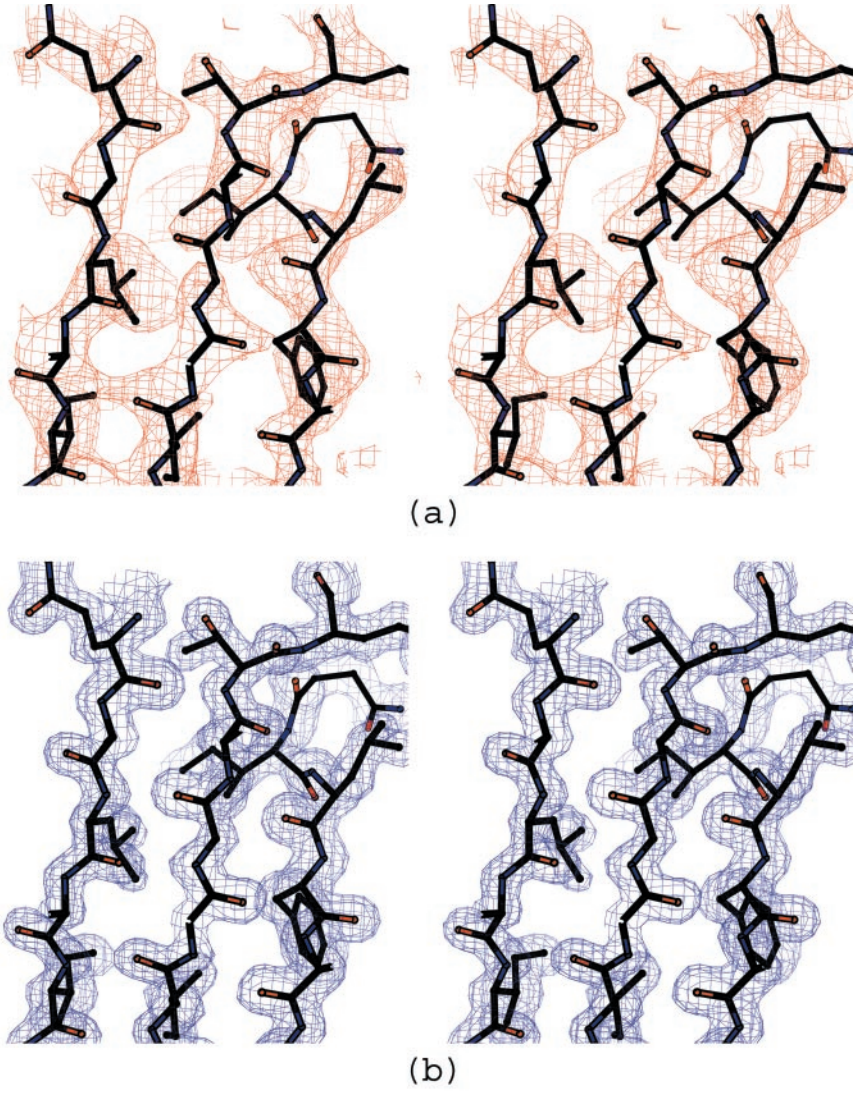

FIG. 1. **Electron density maps of the central β-sheet region of TonB.** *a*, stereoview of the MAD-phased electron density map contoured at 1.0 σ. The map was calculated with phases from the program SOLVE (42), modified with DM (44). *b*, stereoview of the final $2F_o - F_c$ map calculated with the program SHELX (48), contoured at 1.5 σ.

swapped between the monomers (Fig. 2). Four β-strands, S1 and S3 of both molecules, are located on one side, whereas the two short β-strands S2 and the helices are located on the other side (Fig. 3).

The two monomers differ slightly from each other. At any refinement stage, application of non-crystallographic restraints between the two molecules resulted in significantly worse behavior than if such restraints were not utilized. The r.m.s. deviation between the Cα atoms of the two monomers is 0.42 Å, whereas the r.m.s. deviation between the side-chain atoms of the two monomers is 1.15 Å. In the case of the main chain of the protein, the largest differences are found at the N terminus. As judged by their high temperature factors, both termini are located in highly flexible regions of the structure. The difference between Cα positions of Ala-165, the first visible residue on the N terminus, exceeds 2 Å (residues preceding Ala-165 were not visible in either molecule). In the case of the side chains, several residues show significantly different values of the χ_1 angle. These residues include Leu-170, Arg-171, Glu-173, Asn-200, Lys-219, and Lys-231. The only hydrophobic amino acid among them is Leu-170, and different orientation of its side chain leads to the presence of more hydrophobic contacts in molecule B. The other residues are all polar or charged, and all are solvent-exposed. The orientations of the Cγ atoms in the residues belonging to the β-sheet (Arg-171, Glu-173, Lys-231) closely coincide. For positively charged residues (Arg-171 and Lys-231 of both molecules) Cγ atoms point toward the N terminus of molecule A. The Cγ atoms of the negatively charged residue Glu-173 point toward the N terminus of molecule B. Asn-200 is located just after the highly flexible loop and is itself flexible, judged by its high *B*-factor. Lys-219 is located at the end of the molecule and is also flexible.

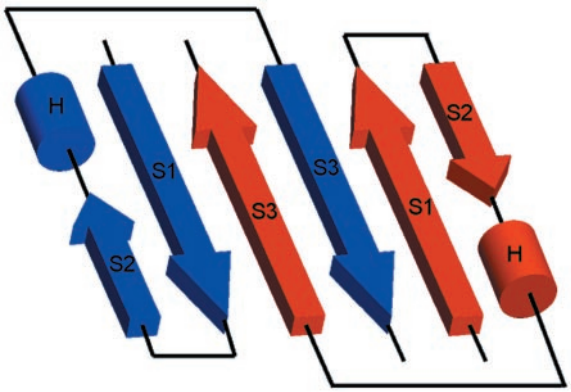

FIG. 2. **Schematic diagram of the secondary structure topology of the C-terminal domain of TonB.** Molecule A is colored in *red* and molecule B in *blue*. The *arrows* represent β strands, and each *cylinder* represents a helix. The secondary structure elements are labeled, and the residues belonging to each of them are described in the text.

The interactions between the two protein chains that form a single compact molecule of the C-terminal domain of TonB are unusually extensive. The dimeric interface area covers 41% of the surface of each monomer, thus the individual chains are unlikely to be able to exist independently and the protein becomes stable only as a dimer. The region of the β-sheet shows tight dimeric interactions, whereas the interactions on the opposite side of the molecule are not as close. Although the single antiparallel β-sheet present in the dimer is composed of strands originating from different molecules, the hydrogen bonding pattern is close to ideal. The loop between β-strand S2 and the α-helix is very flexible, as indicated by its high *B*-factor. The average *B*-factors of the main-chain atoms in this loop are 71 $Å^2$ and 60 $Å^2$ for molecules A and B, respectively, as compared with the respective averages for other areas of 20.6 $Å^2$ and 21.7 $Å^2$. Crystal packing in the vicinity of these loops is rather loose, resulting in the formation of clefts or channels on the molecular surface. The channels are made by residues 195–200 and 172–176 in both molecules, the former belonging to the loop, and the latter to the β-strand S1.

DISCUSSION

The binding of a nutrient, such as vitamin B_{12} or an iron·siderophore complex, to the external face of an outer membrane receptor triggers a series of conformational changes: The N-terminally located TonB box, which is hidden within the barrel of the unliganded receptor, is made to project in an extended form into the periplasm and, thus, becomes freely accessible for interaction with the C-terminal domain of TonB (28). Additionally, subtle structural changes of the receptor observed crystallographically, such as the upward translation of selected loops of the cork domain (also termed "hatch region"), may disrupt hydrophobic interactions between the so-

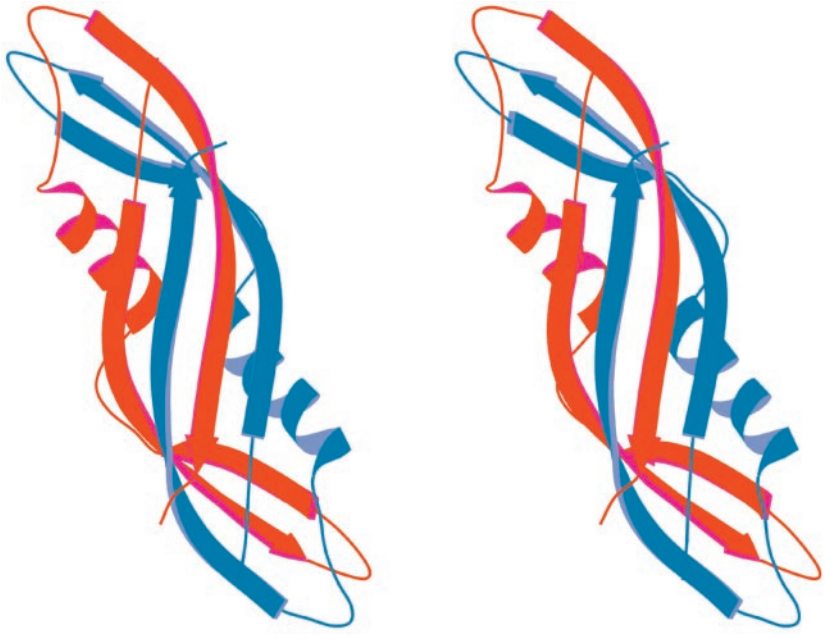

FIG. 3. **Stereo ribbon diagram of the C-terminal domain of TonB, showing the intertwined dimer.** The *color scheme* is the same as in Fig. 2. The atomic coordinates have been deposited in the Protein Data Bank (accession code 1IHR).

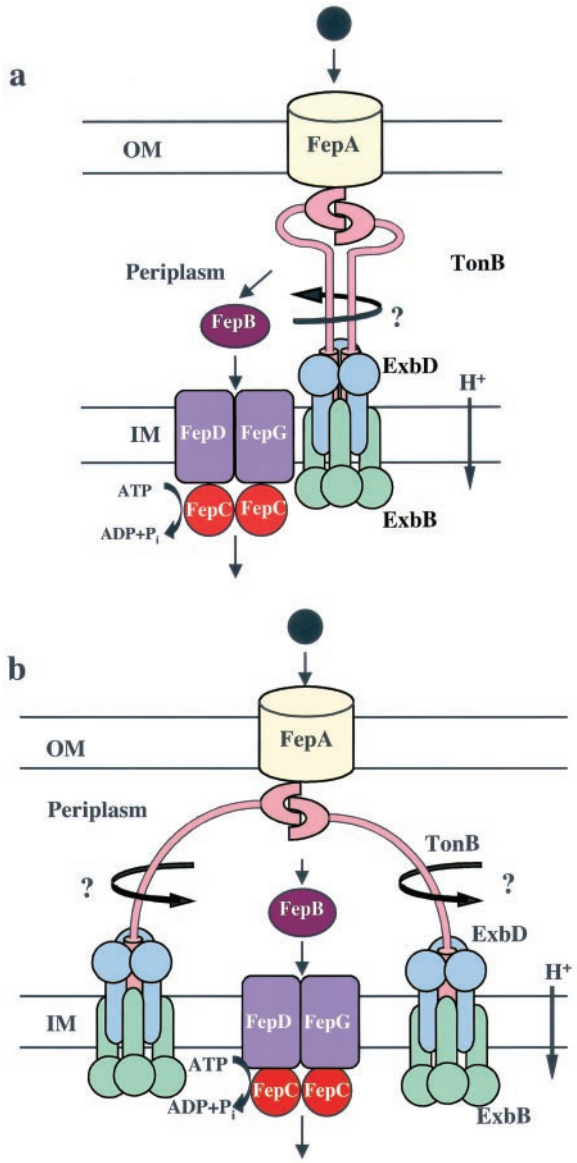

FIG. 4. **Hypothetical models of the interaction of dimeric TonB with (*a*) a single complex of trimeric ExbB·ExbD or (*b*) two complexes of ExbB·ExbD.** For details, see text.

called switch helix (residues 24–29 in FhuA) and the internal wall of the barrel, and the helix unfolds (6). It thus constitutes a candidate for signaling the occupancy of the outer binding site by a ligand to the periplasm. However, the actual "tag" being recognized by TonB could still be the TonB box, the switch helix mediating its accessibility. Nevertheless, there must be additional crucial conformational changes occurring in the barrel itself. Both in FhuA and FepA, the cork domain has been completely deleted and the TonB dependence of transport was fully maintained (32, 33). It follows that TonB must interact with the barrel itself, but this result certainly does not refute an interaction with the TonB box or other regions in the plug domains in wild-type receptors.

It is not clear whether substrate transport normally involves the complete dissociation of the plug domain from the barrel. On the one hand, this does not seem to be necessary, because it is conceivable that channels of sufficient dimension can be created by much smaller movements and changes in the cork domain, even though this is a matter of debate (5, 6). On the other hand, phages can inject their DNA through this pore (34) and colicins use it for entry (34), and this is only conceivable with a completely unplugged pore. Furthermore, the unplugged state is apparently functional (32, 33) and thus able to exist, and therefore a full opening of the pore is likely at least for the entry of very large molecules.

The ligand-mediated signal could therefore trigger a conformational rearrangement first at the loops of the cork domain and the barrel of the receptor which is then transmitted along the barrel. The binding of TonB, which appears to be not continuous but to occur in cycles (12), may then stabilize an intrinsically energetically unfavorable conformation of the barrel, which allows the passage of the ligand. Additionally, TonB may bind to the cork domain in wild-type receptor and help its dislocation, but this is apparently not the decisive action for mediating ligand transport. The binding of TonB to the barrel is needed to effect ligand translocation. The "energizing" of the receptor might then simply consist of the binding of TonB to an intrinsically unstable form of the barrel, which stabilizes this form, allowing the passage of the nutrient, and a subsequent release of the TonB-receptor interaction is needed. We do not know which of these steps would require energy, and it might conceivably be the dissociation of TonB. Although this is ultimately a mechanical act, more sophisticated possibilities exist for a polypeptide machine than simple rigid movement. The barrel domain would then return to its ground state, ready to accept the next ligand molecule. An "energized conformation" of the TonB C-terminal domain would not be required in our model. We consider the possibility (see below) that this transient binding of TonB to the receptor barrel involves a rotary motion in the cytoplasmic membrane.

Cross-linking studies have indicated that the region around residue 160 of TonB is crucial for the interaction with the TonB box (27, 29, 54). In our model, this region is not visible because of its very high flexibility (see the description of the *B*-factors in "Results"). However, it is very likely that other regions of TonB are involved in the contact with the receptor, and it is clear that there must be an interaction with the barrel. Based on NMR studies, it has also been proposed that the C-terminal portion of the proline-rich segment (Lys-Pro repeats) (amino acids 91–102) of TonB is involved in a specific interaction with FhuA (55), but the binding constant is very weak, and this region has been deleted, with TonB still maintaining activity (56). We postulate that the region around Asn-200 of TonB (N terminus of the α helix) constitutes a binding cleft, which could accommodate an element of the receptor as the ligand, based on the relatively high conformational lability of this segment (see "Results"). Interestingly, the α-helix-forming residues (Met-201 through Arg-214) are conserved among several Gram-negative species (14). However, it is unlikely that the role assigned to this otherwise correctly predicted amphipathic helix by Larsen *et al.* (56), namely, binding to the outer membrane, is correct, because the hydrophobic side of this helix faces the core of the dimer and thus cannot participate in any other interactions.

Once the substrate reaches the periplasmic side of the receptor (*e.g.* FepA), it is taken up by the periplasmic-binding protein FepB. The subsequent steps of import are not well known. Substrate-containing FepB might then bind to the ABC transporter $FepC_2DG$, resulting in transport across the inner membrane, using energy derived from ATP hydrolysis (3). FhuA uses an analogous system with FhuD as a periplasmic-binding protein and FhuBC anchored in the inner membrane (57, 58).

In the present work, we provide the first evidence that the C-terminal domain of TonB forms a dimer. However, this dimerization that involves almost half of the surface of this protein domain does not correlate with the recent model, showing a homotrimeric ExbB·ExbD complex interacting with a

TonB monomer, which in turn contacts the OM receptor (21). Furthermore, the antiparallel orientation of each monomer as well as the cylindrical shape do not correspond to any topological representation of TonB described so far in the literature. Recently, a soluble form of TonB was expressed, which lacks the N-terminal anchor helix but contains the full proline-rich region (59). The authors interpreted equilibrium sedimentation and gel filtration data as indicating mostly monomers, even though the measured molecular weight was somewhat higher than expected.

The tightly intertwined dimeric structure of TonB seen in the crystal now leads to two possible, albeit speculative models (Fig. 4). In one case (Fig. 4*a*), both TonB proteins interact with the same ExbB·ExbD complex. It is attractive to hypothesize that the proton gradient might cause a torsional motion, as is found in several molecular machines such as the flagellum or ATP synthases, because of some homology in ExbB to MotA and a similar topology of ExbD to MotB. Two proline-rich regions would provide a stiffer structure than only one, which could thus directly transduce this force to the TonB C-terminal domain and mediate its transient interaction with the receptor barrel and/or the cork domain. Alternatively (Fig. 4*b*), each TonB monomer might be linked to a different ExbB·ExbD complex, yet a torsion of both might still be mechanically transduced to the outer membrane. Postle and co-workers (56) also deleted most of the proline-rich region, yet TonB was still functional. Nevertheless, a torsional mechanism could still be operational in these short-necked constructs. In our model, TonB only needs to bind, and dissociate again, but in a cyclic manner—we cannot distinguish which is the energy-requiring step. Undoubtedly, further work is necessary to test the validity of either model, and particularly the arrangement in the inner membrane needs to be clarified.

One of the goals of this project was to determine if any structural homology exists between the C-terminal domains of TonB and TolA (36). A direct comparison of these domains proves that their structure is completely different. Moreover, a comparison of the structure of TonB with all known protein folds (60) detected no structural relationship between the C-terminal domain of TonB and any other structure represented in the Protein Data Bank. This was true regardless of whether a monomer or a dimer of TonB was utilized as a search model. In this respect, the structure described here represents a totally new fold that has never been observed so far.

In conclusion, the most surprising finding of our structure is that the C-terminal domain of TonB forms a rigid and tightly intertwined dimer. It is conceivable that this is essential for transducing a mechanical force from the inner to the outer membrane, and it would be much harder to imagine this to occur with a monomeric molecule. Even though polyproline stretches have extended conformations, they are still flexible and are typical hinge regions, as exemplified in IgG molecules. It would thus be difficult to visualize how mechanical energy can be transduced with a flexible tether of a monomeric molecule. Our dimeric structure provides now a framework for further probing of the mechanism of the TonB-dependent import.

Acknowledgments—We thank Dr. Z. Dauter for his assistance in data collection on beamline X9B at the National Synchrotron Light Source, Brookhaven National Laboratory, and Dr. P. Forrer for providing the gpD fusion system for use in the expression of TonB.

REFERENCES

1. Schirmer, T. (1998) *J. Struct. Biol.* **121,** 101–109
2. Ehrmann, M., Ehrle, R., Hofmann, E., Boos, W., and Schlosser, A. (1998) *Mol. Microbiol.* **29,** 685–694
3. Buchanan, S. K. (2001) *Trends Biochem. Sci.* **26,** 3–6
4. Buchanan, S. K., Smith, B. S., Venkatramani, L., Xia, D., Esser, L., Palnitkar, M., Chakraborty, R., van der Helm, D., and Deisenhofer, J. (1999) *Nat. Struct. Biol.* **6,** 56–63
5. Ferguson, A. D., Hofmann, E., Coulton, J. W., Diederichs, K., and Welte, W. (1998) *Science* **282,** 2215–2220
6. Locher, K. P., Rees, B., Koebnik, R., Mitschler, A., Moulinier, L., Rosenbusch, J. P., and Moras, D. (1998) *Cell* **95,** 771–778
7. Newton, S. M., Allen, J. S., Cao, Z., Qi, Z., Jiang, X., Sprencel, C., Igo, J. D., Foster, S. B., Payne, M. A., and Klebba, P. E. (1997) *Proc. Natl. Acad. Sci. U. S. A.* **94,** 4560–4565
8. Nikaido, H., and Saier, M. H., Jr. (1992) *Science* **258,** 936–942
9. Jiang, X., Payne, M. A., Cao, Z., Foster, S. B., Feix, J. B., Newton, S. M., and Klebba, P. E. (1997) *Science* **276,** 1261–1264
10. Reynolds, P. R., Mottur, G. P., and Bradbeer, C. (1980) *J. Biol. Chem.* **255,** 4313–4319
11. Wooldridge, K. G., Morrissey, J. A., and Williams, P. H. (1992) *J. Gen. Microbiol.* **138,** 597–603
12. Larsen, R. A., Thomas, M. G., and Postle, K. (1999) *Mol. Microbiol.* **31,** 1809–1824
13. Letain, T. E., and Postle, K. (1997) *Mol. Microbiol.* **24,** 271–283
14. Larsen, R. A., Myers, P. S., Skare, J. T., Seachord, C. L., Darveau, R. P., and Postle, K. (1996) *J. Bacteriol.* **178,** 1363–1373
15. Postle, K., and Skare, J. T. (1988) *J. Biol. Chem.* **263,** 11000–11007
16. Karlsson, M., Hannavy, K., and Higgins, C. F. (1993) *Mol. Microbiol.* **8,** 379–388
17. Larsen, R. A., and Postle, K. (2001) *J. Biol. Chem.* **276,** 8111–8117
18. Skare, J. T., Ahmer, B. M., Seachord, C. L., Darveau, R. P., and Postle, K. (1993) *J. Biol. Chem.* **268,** 16302–16308
19. Larsen, R. A., Foster-Hartnett, D., McIntosh, M. A., and Postle, K. (1997) *J. Bacteriol.* **179,** 3213–3221
20. Larsen, R. A., Thomas, M. G., Wood, G. E., and Postle, K. (1994) *Mol. Microbiol.* **13,** 627–640
21. Higgs, P. I., Myers, P. S., and Postle, K. (1998) *J. Bacteriol.* **180,** 6031–6038
22. Braun, V. (1995) *FEMS Microbiol. Rev.* **16,** 295–307
23. Hancock, R. W., and Braun, V. (1976) *J. Bacteriol.* **125,** 409–415
24. Bradbeer, C. (1993) *J. Bacteriol.* **175,** 3146–3150
25. Schramm, E., Mende, J., Braun, V., and Kamp, R. M. (1987) *J. Bacteriol.* **169,** 3350–3357
26. Gudmundsdottir, A., Bell, P. E., Lundrigan, M. D., Bradbeer, C., and Kadner, R. J. (1989) *J. Bacteriol.* **171,** 6526–6533
27. Cadieux, N., and Kadner, R. J. (1999) *Proc. Natl. Acad. Sci. U. S. A.* **96,** 10673–10678
28. Merianos, H. J., Cadieux, N., Lin, C. H., Kadner, R. J., and Cafiso, D. S. (2000) *Nat. Struct. Biol.* **7,** 205–209
29. Cadieux, N., Bradbeer, C., and Kadner, R. J. (2000) *J. Bacteriol.* **182,** 5954–5961
30. Moeck, G. S., Coulton, J. W., and Postle, K. (1997) *J. Biol. Chem.* **272,** 28391–28397
31. Postle, K. (1993) *J. Bioenerg. Biomembr.* **25,** 591–601
32. Braun, M., Killmann, H., and Braun, V. (1999) *Mol. Microbiol.* **33,** 1037–1049
33. Scott, D. C., Cao, Z., Qi, Z., Bauler, M., Igo, J. D., Newton, S. M., and Klebba, P. E. (2001) *J. Biol. Chem.* **276,** 13025–13033
34. Lazdunski, C. J., Bouveret, E., Rigal, A., Journet, L., Lloubes, R., and Benedetti, H. (1998) *J. Bacteriol.* **180,** 4993–5002
35. Eick-Helmerich, K., and Braun, V. (1989) *J. Bacteriol.* **171,** 5117–5126
36. Lubkowski, J., Hennecke, F., Plückthun, A., and Wlodawer, A. (1999) *Structure* **7,** 711–722
37. Forrer, P., and Jaussi, R. (1998) *Gene* **224,** 45–52
38. Plückthun, A., Krebber, A., Krebber, C., Horn, U., Knüpfer, U., Wenderoth, R., Nieba, L., Proba, K., and Riesenberg, D. (1996) in *Antibody Engineering: A Practical Approach* (McCafferty, J., and Hoogenboom, H. R., eds) pp. 203–252, IRL Press, Oxford
39. Dauter, Z., Dauter, M., and Rajashankar, K. R. (2000) *Acta Crystallogr. Sect. D Biol. Crystallogr.* **56,** 232–237
40. Dauter, Z., Li, M., and Wlodawer, A. (2001) *Acta Crystallogr. Sect. D Biol. Crystallogr.* **57,** 239–249
41. Otwinowski, Z., and Minor, W. (1997) *Methods Enzymol.* **276,** 307–326
42. Terwilliger, T. C., and Berendzen, J. (1996) *Acta Crystallogr. Sect. D Biol. Crystallogr.* **52,** 749–757
43. Sheldrick, G. M. (1997) *Methods Enzymol.* **276,** 628–641
44. Cowtan, K., and Main, P. (1998) *Acta Crystallogr. Sect. D Biol. Crystallogr.* **54,** 487–493
45. Collaborative Computational Project Number 4. (1994) *Acta Crystallogr. Sect. D Biol. Crystallogr.* **50,** 760–763
46. Perrakis, A., Morris, R., and Lamzin, V. S. (1999) *Nat. Struct. Biol.* **6,** 458–463
47. Jones, T. A., and Kieldgaard, M. (1997) *Methods Enzymol.* **277,** 173–208
48. Sheldrick, G. M., and Schneider, T. R. (1997) *Methods Enzymol.* **277,** 319–343
49. Laskowski, R. A., MacArthur, M. W., Moss, D. S., and Thornton, J. M. (1993) *J. Appl. Crystallogr.* **26,** 283–291
50. Hutchinson, E. G., and Thornton, J. M. (1996) *Protein Sci.* **5,** 212–220
51. Kraulis, P. J. (1991) *J. Appl. Crystallogr.* **24,** 946–950
52. Esnouf, R. M. (1999) *Acta Crystallogr. Sect. D Biol. Crystallogr.* **55,** 938–940
53. Meritt, E. A., and Murphy, M. E. P. (1994) *Acta Crystallogr. Sect. D Biol. Crystallogr.* **50,** 869–873
54. Kadner, R. J. (1990) *Mol. Microbiol.* **4,** 2027–2033
55. Brewer, S., Tolley, M., Trayer, I. P., Barr, G. C., Dorman, C. J., Hannavy, K., Higgins, C. F., Evans, J. S., Levine, B. A., and Wormald, M. R. (1990) *J. Mol. Biol.* **216,** 883–895
56. Larsen, R. A., Wood, G. E., and Postle, K. (1993) *Mol. Microbiol* **10,** 943–953
57. Braun, V., Hantke, K., and Köster, W. (1998) in *Metal Ions in Biological Systems: Iron Transport and Storage in Microorganisms, Plants and Animals* (Sigel, A., and Sigel, H., eds) pp. 67–145, Marcel Dekker, New York
58. Groeger, W., and Koster, W. (1998) *Microbiology* **144,** 2759–2769
59. Moeck, G. S., and Letellier, L. (2001) *J. Bacteriol.* **183,** 2755–2764
60. Holm, L., and Sander, C. (1993) *J. Mol. Biol.* **233,** 123–138